



**Flux Density and Power Loss Distribution in  
100kVA Distribution Transformer Core  
Assembled with Different Cutting Angle of  
T-Joint**

By

**Shuhaimi Bin Zakaria @ Abdullah  
0430910015**

A thesis submitted in fulfillment of the requirements for the degree of  
Master of Science (Electrical Systems)

**School of Electrical Systems Engineering  
UNIVERSITI MALAYSIA PERLIS**

**2010**

# UNIVERSITI MALAYSIA PERLIS

## DECLARATION OF THESIS

Author's full name : Shuhaimi Bin Zakaria @ Abdullah  
Date of birth : 7 April 1970  
Title: Flux density and power loss distribution in 100kVA  
distribution transformer core assembled with 60° T-joint  
compared to other different types of T-Joint.  
Academic Session : 2009-2010

I hereby declare that the thesis becomes the property of Universiti Malaysia Perlis (UniMAP) and to be placed at the library of UniMAP. This thesis is classified as:

CONFIDENTIAL { Contains confidential information under the Official Secret Act 1972 }

RESTRICTED { Contains restricted information as specified by the organization where research was done }

OPEN ACCESS I agree that my thesis is to be made immediately available as hard copy or on-line open access (full text)

I, the author, give permission to the UniMAP to reproduce this thesis in whole or in part for the purpose of research or academic exchange only (except during a period of 10 years, if so requested above).

Certified by:

\_\_\_\_\_  
SIGNATURE

Shuhaimi Bin Zakaria @ Abdullah

IC. NO. = 700407095011

Date:

\_\_\_\_\_  
SIGNATURE OF SUPERVISOR

Prof. Dr. Ismail Bin Daut

Date:

## Acknowledgements

The work has been carried out at the School of Electrical System Engineering, Universiti Malaysia Perlis.

I would like to express my gratitude to Professor Dr. Ismail Bin Daut who supervised and also for the guidance and valuable discussion during the research.

Special thank to Professor Madya Dr. Soib Bin Taib from Universiti Sains Malaysia, for the incessant encouragement and also for valuable discussion.

I would like to thank En. Shahanom Bin Uthman, Malaysian Transformer Manufacturing and TNB Research for the providing of the 1000kVA Distribution Transformer core and the grain oriented silicon steel (CRGO 3% Si-Fe), for commercial name known as M5 used in this research.

I am grateful to all the staff and students at the School of Electrical System Engineering, Universiti Malaysia Perlis for their help, discussion and friendly atmosphere throughout my studies.

Finally, I would like to appreciate the inestimable support, patience and encouragement which I received from my family.

## Table of Contents

<b>Acknowledgements</b> .....	iii
<b>Table Of Contents</b> .....	iv
<b>List Of Tables</b> .....	viii
<b>List Of Figures</b> .....	ix
<b>List Of Symbols</b> .....	xiv
<b>Abstrak</b> .....	xvii
<b>Abstract</b> .....	xviii
<b>Chapter One – Introduction</b> .....	1
1.1 Introduction .....	1
1.2 The Aim Of This Research .....	2
<b>Chapter Two - Magnetic Properties, Flux Distributions And Losses</b> .....	3
2.1 Magnetic Properties Of The Ferromagnetic materials .....	3
2.1.1. The Magnetisation And Domain Theory .....	3
2.1.2. Magnetisation Curve .....	5
2.1.3 Demagnetising Field .....	6
2.1.4 Magnetocrystalline Anisotropy .....	6
2.1.5 The Magnetism And Rotational Magnetisation .....	7
2.1.6 The Alternating Magnetisation .....	9
2.1.7 The Rotational Magnetisation .....	12
2.1.8 The Soft Magnetic Materials Subjected To The Rotational Magnetisation .....	13
2.2 Flux Distribution .....	14
2.2.1 The Excitation Current .....	14
2.2.2 The Core Geometry And Flux Distribution .....	15
2.2.3 Inplane Flux Distribution .....	16
2.2.4 Interlaminar Flux .....	17
2.2.5 The Influence Of The Type Of The Joint .....	18
2.2.6 The Effects Of The Air Gaps And Overlap Length .....	20

2.3	The Losses .....	22
2.3.1	The Hysteresis Loss .....	22
2.3.2	The Eddy Current Loss .....	24
2.3.3	The No-Load Losses .....	25
2.3.4	The Power Losses Under The Alternating Magnetisation .....	25
2.3.5	The Power Losses Under The Rotational Magnetisation .....	27
<b>Chapter Three - The Experimental Measurement Technique .....</b>		<b>30</b>
3.1	Overall Power Loss Measurement .....	30
3.2	Power Loss Measurement Technique .....	32
3.3	The Search Coil Technique .....	33
3.4	The Localised Flux Density Measurement .....	38
3.5	The Epstein Tester Technique .....	40
3.6	The Thermistor Technique .....	42
3.7	The QuickField Software Technique .....	44
3.8	The Matlab Software Technique .....	46
<b>Chapter Four - Experimental And Measurement Procedure .....</b>		<b>47</b>
4.1	The No-Load Loss Measurement .....	47
4.2	Measurement Sequence .....	49
4.3	The Transformer Core For The No-Load Loss .....	50
4.4	The Model Core Assembled With The 90° T-Joint .....	50
4.5	The Model Core Assembled With The 60° T-Joint .....	56
4.6	The Model Core Assembled With The 45° T-Joint .....	59
4.7	The Model Core Assembled With The 23° T-Joint .....	62
<b>Chapter Five - Experimental Results .....</b>		<b>65</b>
5.1	Nominal Loss Of The Grain Oriented Silicon Steel (M5) .....	65
5.2	The Power Loss And The Building Factor Of The Core Assembled With The Butt Lap Joint .....	66
5.3	The Power Loss And The Building Factor Result Of The Core Assembled With The 60° T-joint .....	67
5.4	The Power Loss And The Building Factor Of The Core Assembled With The 45° T-joint .....	68
5.5	The Power Loss And The Building Factor Of The Core Assembled With the 23° T-joint .....	69

5.6.	The Localised Flux Density Using The Search Coil .....	71
5.6.1.	The Flux Of The Localised Flux Density At The Corner Joint .....	71
5.6.2.	The Flux Of The Localised Flux Density At The Butt Lap Joint .....	72
5.6.3.	The Flux Of The Localised Flux Density At The 60° T-joint .....	74
5.6.4.	The Flux Of The Localised Flux Density At The 45° T-Joint .....	75
5.6.5.	The Flux Of The Localised Flux Density At The 23° T-Joint .....	76
5.7.	The Localised Power Loss Measurement Using The Thermistor .....	78
5.7.1.	The Localised Power Loss At The Corner Joint .....	78
5.7.2.	The Localised Power Loss At The Butt Lap Joint .....	79
5.7.3.	The Localised Power Loss At The 60° T-Joint .....	80
5.7.4.	The Localised Power Loss At The 45° T-Joint .....	81
5.7.5.	The Localised Power Loss At The 23° T-Joint .....	82
<b>Chapter Six - Discussion Of The Results .....</b>		<b>84</b>
6.1	The Building Factor (B.F) .....	84
6.2	The Power Loss Of The Different Transformer Core .....	85
6.3	The Localised Flux Density At The Corner Joint .....	90
6.3.1.	The Localised Flux Density Of The Fundamental Harmonic .....	90
6.3.2.	The Localised Flux Density Of The Third Harmonic .....	92
6.3.3.	The Localised Flux Density Of The Fifth Harmonic .....	95
6.3.4.	The Normal Flux Density Of The Fundamental Harmonic .....	97
6.4	The Localised Power Loss At The Corner Joint .....	98
6.5	The Localised Flux Density At The T-Joint .....	100
6.5.1.	The Localised Flux Density Of The Fundamental Harmonic .....	100
6.5.2.	The Localised Flux Density Of The Third Harmonic .....	102
6.5.3.	The Localised Flux Density Of The Fifth Harmonic .....	104
6.5.4.	The Normal Flux Density Of The Fundamental Harmonic .....	106
6.6	The Localised Power Loss At The T-Joint .....	108

<b>Chapter Seven - Conclusions</b> .....	111
7.1 Conclusions .....	111
7.2 The Advantages .....	113
7.3 The Disadvantages .....	114
7.4 Recommendation For The Future Work .....	114
7.5 Economical Aspects .....	115
<b>References</b> .....	118
<b>Appendices</b>	

© This item is protected by original copyright

## LIST OF TABLES

2.1	The maximum values of the relative permeability, $\mu_r$ for some paramagnets, diamagnets and ferromagnets. ....	9
6.1	The percentage of the B.F in the model core assembled with all four types of the T-joint compared to the Butt Lap joint model magnetised with 1.5 T .....	84
6.2	The percentage of the power loss in the model core assembled with all four types of the T-joint compared to the Butt Lap joint model magnetised with 1.5T .....	86
7.1	Transformer that purchased by TNBD from 1999 to 2008.....	115
7.2	The losses of the transformer assembled with the Butt Lap joint per day....	116
7.3	The losses of the transformer assembled with the 60° T-joint per day.....	116
7.4	The total loss per day when using the transformer assembled with the Butt Lap joint.....	116
7.5	The total loss per day when using the transformer assembled with the 60° T-joint.....	117
7.6	The total RM saved per day and total RM saved per year when using the transformer assembled with the 60° T-joint.....	117



## LIST OF FIGURES

2.1	Domain processes occurring as a material is magnetised to saturation. ....	4
2.2	Domain wall structure of M5 magnify by 500X.....	4
2.3	Domain wall structure of M5 magnify by 300X.....	5
2.4	The B versus H curve of the ferromagnetic material. ....	5
2.5	Magnetisation curves for the magnetocrystalline anisotropy of the iron. ....	7
2.6	Typical magnetisation curves for the paramagnets and the diamagnets. ....	9
2.7	The explanation of energy minimisation in ferromagnets.....	10
2.8	The changes in domain structure as the material is magnetised up to saturation.....	12
2.9	The B-H loop of the ferromagnets. ....	12
2.10	The rotational magnetisation at the T-joint of the three limb transformer core. ....	13
2.11	Differences in magnetic path lengths, I and II. ....	16
2.12	Instantaneous flux streamlines when the flux in the center limb is maximum.....	17
2.13	The typical normal flux density magnitudes. ....	18
2.14	Types of T-joints in laminated cores. ....	19
2.15	Types of T-joint that use for the transformer model.....	20
2.16	Side view of the mitred joint showing the saturated bridging region. ....	21
2.17	Typical hysteresis loop .....	23
2.18	The concept of separating the power loss into hysteresis and eddy currents components.....	27
2.19	Three types of magnetisation.....	28
2.20	The rotational magnetisation and the orthogonal components of the magnetic field and flux density. ....	28
2.21	The comparison of the power loss characteristics for the alternating and the rotational magnetisation. ....	29
3.1	The diagram of the measuring circuit. ....	31
3.2	The diagram of the methods that used to measure the localised flux density and the localised power loss. ....	31
3.3	The power loss measurement set-up on the transformer model core.....	32
3.4	The power loss measurement set-up on the lamination sample using the Single Sheet Tester.....	33
3.5	The concept of the search coil technique. ....	35

3.6	The concept of the search coil measuring localised flux density.....	35
3.7	The specimen with a pair of perpendicular search coils. ....	35
3.8	The dimensions of the hole drilled in the specimen.....	36
3.9	The search coil connect to the meter with connecting wires are not twisted and create unintentional loop. ....	37
3.10	The search coil connect to the meter with connecting wires are twisted in order to minimise the influence of the stray magnetic field. ....	37
3.11	The twisted and short circuit connecting wires. ....	37
3.12	The locations of the search coils at the T-joint. ....	39
3.13	The locations of the search coils at the corner joint.....	39
3.14	The mesh graph of the localised flux density measured by the search coil. ....	39
3.15	The sample layout of 50cm Epstein Tester frame. ....	41
3.16	The layout of the Baby 25cm Epstein Tester frame. ....	41
3.17	The circuit diagram for the Epstein Tester frame. ....	41
3.18	The locations of the thermistor at the T-joint. ....	43
3.19	The locations of the thermistor at the corner joint. ....	43
3.20	The example mesh graph of the localised power loss measured by the thermistor using Matlab Software.....	43
3.21	The direction of the magnetic flux flows at the Butt Lap and 23° T-joint. ....	44
3.22	The direction of the magnetic flux flows at the 45° and 60° T-joint. ....	45
3.23	The magnetic flux flows at the Butt Lap and 23° T-joint using the QuickField Software ....	45
3.24	The magnetic flux flows at the 45° and 60° T-joint using the QuickField Software. ....	45
3.25	The mesh graph of the localised flux density or power loss at the lamination. ....	46
3.26	The mesh and contour graph of the localised flux density or power loss at the lamination using the Matlab Software.....	46
4.1	The circuit diagram of the conventional method test for the No-Load loss measurements. ....	48
4.2	The circuit diagram of the modern test. ....	48
4.3	The dimensional of the model core assembled with the Butt Lap joint. ....	51
4.4	The platforms used for the model core assembled with the Butt Lap joint. ....	51
4.5	The connection circuit for the model core assembled with the Butt Lap joint. ....	53
4.6	The equipment that use in the search coils method. ....	54

4.7	The circuit that use in the thermistor method. ....	54
4.8	The equipment that use in the thermistor method. ....	54
4.9	The measuring point location of the search coil and the thermistor at the corner and Butt Lap joint. ....	55
4.10	The measuring point location of the search coil and the thermistor on the model core assembled with the Butt Lap joint. ....	55
4.11	The dimensional of the model core assembled with the 60° T-joint.....	56
4.12	The platforms used for the model core assembled with the 60° T-joint. ....	56
4.13	The connection circuit for the model core assembled with the 60° T-joint....	57
4.14	The measuring point location of the search coil and the thermistor at the 60° T-joint.....	58
4.15	The location of the search coil and the thermistor on the model core assembled with the 60° T-joint.....	58
4.16	The dimensional of the model core assembled with the 45° T-joint. ....	59
4.17	The platforms used for the model core assembled with the 45° T-joint. ....	59
4.18	The connection circuit for the model core assembled with the 45° T-joint....	60
4.19	The measuring point location of the search coil and the thermistor at the 45° T-joint. ....	61
4.20	The location of the search coil and the thermistor on the model core assembled with the 45° T-joint. ....	61
4.21	The dimensional of the model core assembled with the 23° T-joint.....	62
4.22	The platforms used for the model core assembled with the 23° T-joint.....	62
4.23	The connection circuit for the model core assembled with the 23° T-joint....	63
4.24	The measuring point location of the search coil and the thermistor at the 23° T-joint. ....	65
4.25	The location of the search coil and the thermistor on the model core assembled with the 23° T-joint.....	64
5.1	The graph of the nominal loss from the Epstein and Iron Loss Tester.....	66
5.2	The graph of the power loss on the model core assembled with the Butt Lap joint. ....	66
5.3	The graph of the B.F on the model core assembled with the Butt Lap joint. ....	67
5.4	The graph of the power loss on the model core assembled with the 60° T-joint.....	67
5.5	The graph of the B.F on the model core assembled with the 60° T-joint.....	68
5.6	The graph of the power loss on the model core assembled with the 45° T-joint. ....	69

5.7	The graph of the B.F on the model core assembled with the 45° T-joint .....	69
5.8	The graph of the power loss on the model core assembled with the 23° T-joint .....	70
5.9	The graph of the B.F on the model core assembled with the 23° T-joint .....	70
5.10	The mesh and contour graph of the localised flux density measured by the search coil at the corner joint magnetised with 1.5 T .....	72
5.11	The mesh and contour graph of the localised flux density measured by the search coil on the model core assembled with the Butt Lap joint magnetised with 1.5 T .....	73
5.12	The mesh and contour graph of the localised flux density measured by the search coil on the model core assembled with the 60° T-joint magnetised with 1.5 T .....	74
5.13	The mesh and contour graph of the localised flux density measured by the search coil on the model core assembled with the 45° T-joint magnetised with 1.5 T .....	76
5.14	The mesh and contour graph of the localised flux density measured by the search coil on the model core assembled with the 23° T-joint magnetised with 1.5 T .....	77
5.15	The mesh and contour graph of the localised power loss measured by the thermistor at the corner joint magnetised with 1.5 T .....	79
5.16	The mesh and contour graph of the localised power loss using the thermistor on the model core assembled with the Butt Lap joint magnetised with 1.5 T .....	80
5.17	The mesh and contour graph of the localised power loss measured by the thermistor on the model core assembled with the 60° T-joint magnetised with 1.5 T .....	81
5.18	The mesh and contour graph of the localised power loss measured by the thermistor on the model core assembled with the 45° T-joint magnetised with 1.5 T .....	82
5.19	The mesh and contour graph of the localised power loss measured by thermistor on the model core assembled with the 23° T-joint magnetised with 1.5 T .....	83
6.1	The graphs of the B.F for all models T-joint .....	85
6.2	The graphs of the power loss for the transformer cores assembled with the different T-joint.....	87

6.3	The direction of the flux flows at the T-joint .....	88
6.4	The side view of the flux flows at the joint .....	89
6.5	The direction of the flux flows at the corner joint .....	89
6.6	The overlap length of the T-joint .....	90
6.7	The mesh and contour graph of the localised flux density measured by the search coil at the corner joint magnetised with 1.5 T .....	92
6.8	The mesh graph of the local variations in mT of the third harmonic peak flux density in the lamination in the corner joint at 1.5 T .....	94
6.9	The mesh and contour graph of the local variations in mT of the fifth harmonic peak flux density in the lamination in the corner joint at 1.5 T .....	96
6.10	The mesh and contour graph of the local variations in mT of the normal flux density in the corner joint at 1.5 T .....	97
6.11	The mesh and contour graph of the localised power loss measured by the thermistor at the corner joint magnetised with 1.5 T .....	99
6.12	The mesh graph of the localised flux density measured by the search coil at all four types of the T-joint magnetised with 1.5 T.....	101
6.13	The contour graph of the localised flux density measured by the search coil at all four types of the T-joint magnetised with 1.5 T.....	102
6.14	The mesh graph of the local variations in mT of the third harmonic flux in the lamination in different T-joint at 1.5 T.....	103
6.15	The contour graph of the local variations in mT of the third harmonic flux in the lamination in different T-joint at 1.5 T .....	104
6.16	The mesh graph of the local variations in mT of the fifth harmonic flux in the lamination in the different T-joint at 1.5 T .....	105
6.17	The contour graph of the local variations in mT of the fifth harmonic flux in the lamination in the different T-joint at 1.5 T.....	106
6.18	The mesh graph of the local variations in mT of the normal flux in the lamination in the different T-joint at 1.5 T .....	107
6.19	The contour graph of the local variations in mT of the normal flux in the lamination in the different T-joint at 1.5 T .....	107
6.20	The mesh graph of the localised power loss measured by the thermistor at all four types of the T-joint magnetised with 1.5 T. ....	109
6.21	The contour graph of the localised power loss measured by the thermistor at all four types of the T-joint magnetised with 1.5 T. ....	110

## List Of Symbols

$B$	Maximum flux density in the core in Tesla
$B_r$	Remanence or residual flux density
$B_{\text{peak}}$	A peak flux density
$B_{\text{max}}$	Maximum flux density
$B_m$	Flux magnitude
$B_c$	Flux magnitude of circular
$B_x$	flux in x direction
$B_y$	flux in y direction
$H$	Magnetic field strength
M5	Grain oriented silicon steel sheet's grade
$\mu$	Permeability
$\mu_{\text{in}}$	Initial permeability
$\mu_m$	Maximum permeability
$\mu_0$	Permeability of free space
$\mu_r$	Relative permeability
A/m	Magnetic field strength unit
H/m	Permeability of free space unit
$H_{\text{in}}$	Internal magnetic field strength
$H_{\text{app}}$	Applied magnetic field strength
$H_d$	Demagnetising field strength
$H_c$	Coercive force
$H_x$	Magnetic field strength in x direction
$H_y$	Magnetic field strength in y direction
$N_d$	Demagnetising factor
M	Magnetisation of material
f	Frequency in hertz
V	Voltage
T	Tesla
W	Watt
J	Polarization
$J_r$	Residual polarization
Fe	Iron

Co	Cobalt
Ni	Nickel
S	Overlap region
g	Air gap length
a	Overlap length
$\Phi_g$	Flux air gap
$\Phi_s$	Flux overlap
$W_H$	Energy
$W_E$	Excess loss
k	Constant
$W_{n\text{classical}}$	Classical eddy current loss
t	Sheet thickness
$\beta$	Geometrical factor
$\rho$	Resistivity
$P_e$	Eddy current loss
$P_{\text{tot}}$	Total power loss
$P_h$	Hysteresis loss
$P_a$	Anomalous loss
D	Density
d	Thickness
L	Live
N	Neutral
$L_1$	Live 1
$L_2$	Live 2
$L_3$	Live 3
$L_R$	Live red
$L_Y$	Live yellow
$L_B$	Live blue
$I_p$	Primary current
$V_s$	Secondary voltage
R	Red phase
Y	Yellow phase
B	Blue phase
$I_{PR}$	Primary current red

$I_{PY}$	Primary current yellow
$I_{PB}$	Primary current blue
$V_{SR}$	Secondary voltage red
$V_{SY}$	Secondary voltage Yellow
$V_{SB}$	Secondary voltage blue
Ch1	Oscilloscope channel 1
Ch2	Oscilloscope channel 2
$N$	Number of turn
$A$	Cross section area
$dB/dt$	Rate change of flux density
$V_{rms}$	RMS Voltage
$V_{ave}$	Average voltage
CT	Current transformer
V	Voltmeter
A	Ammeter
W	Wattmeter
G	Alternator
741	Operational amplifier IC
ADC	Analog to Digital convertor IC
LCD	Display type
8085	Microcontroller IC
Kg	Kilogram
W	Watt
W/Kg	Watt/Kilogram
AC	Alternating Current
DC	Direct Current
RM	Ringgit Malaysia
B.F	Building factor
FEM	Finite Element Method
TNB	Tenaga Nasional Berhad
TNBD	Tenaga Nasional Berhad Distribution
SESCO	Sabah Electricity Supply Company



# **Pembahagian Ketumpatan Fluks Dan Kehilangan Kuasa Pada Teras Alat Pengubah Pembahagian 100kVA Sambungan-T Yang Berbeza Sudut**

## **Abstrak**

Kehilangan kuasa yang terhasil daripada permagnetan telah mendapat perhatian sejak dari dahulu lagi. Alat pengubah yang dibina daripada sambungan-T Butt Lap menghasilkan kehilangan kuasa paling tinggi. Ini kerana fluks terpaksa berpusing arah sebanyak  $90^\circ$  di dalam kawasan arah susah dan perlu naik dan turun ke lapisan bersebelahan menyebabkan kehilangan kuasa yang tinggi terhasil pada sambungan-T ini. Untuk mengatasi masalah ini, beberapa jenis potongan bersudut seperti  $23^\circ$ ,  $45^\circ$  dan  $60^\circ$  diperkenalkan di dalam usaha untuk menghasilkan rekabentuk yang lebih baik. Pembinaan model teras alat pengubah pembahagian 100kVA untuk pengukuran kehilangan kuasa dan faktor pembinaan telah dibuat dan eksperimen telah dilakukan untuk menunjukkan sambungan-T yang mana dapat memberikan kehilangan kuasa paling minima dan faktor pembinaan terbaik. Ketumpatan fluks setempat diukur dengan menggunakan "search coil" untuk menunjukkan pembahagian ketumpatan flux setempat pada sambungan tepi dan sambungan-T. Ketumpatan fluks harmonik asas, fluks harmonik ketiga dan fluks harmonik kelima pada fluks normal dan fluks inplane telah diukur di sambungan tepi dan sambungan-T. Kehilangan kuasa setempat diukur dengan menggunakan "thermistor" pada lokasi yang sama dengan "search coil". Keputusan menunjukkan bahawa kehilangan kuasa paling minima, faktor pembinaan terbaik, ketumpatan fluks untuk fluks normal, fluks harmonik asas, fluks harmonik ketiga, fluks harmonik kelima pada fluks normal dan fluks inplane serta kehilangan kuasa setempat adalah paling rendah pada model teras alat pengubah sambungan-T  $60^\circ$ .

# **Flux Density And Power Loss Distribution In 100kVA Distribution Transformer Core Assembled With Different Cutting Angle Of T-Joint**

## **Abstract**

The power losses occurring under magnetising condition have received a great deal of attention for a long time. The transformer designs with Butt Lap joint cause the highest power loss at the T-joint. These due to the flux need to rotate  $90^\circ$  into the hard direction and transfer up and down to the adjacent layers causes high rotational power loss occurred at the T-joint. To overcome this problem, the different cutting angle such as  $23^\circ$ ,  $45^\circ$  and  $60^\circ$  at the T-joint was introduces in order to find out the most efficient design. The development of the 100kVA Distribution Transformer model core with the four difference types of the T-joint for the power loss and building factor measurement has been tested in order to find which T-joint has minimum power loss and better building factor. The localised flux density was measured using the search coil in order to find out their distribution at the corner joint and T-joint. The fundamental, third and fifth harmonic in the normal and inplane flux density were measured at the corner joint and T-joint. The localised power loss was measured using the thermistor at the similar location of the search coil. The results show that the minimum power loss, better building factor, the minimum fundamental, third and fifth harmonic the normal and inplane flux density and also minimum localised power loss are occurred at the transformer model core assembled with the  $60^\circ$  T-joint.

© This item is protected by copyright law

# Chapter One

## Introduction

### 1.1. Introduction

For a long time industry and academia have been working to improve the methods for predicting losses in the laminated transformer cores. The important research findings have been reported over the last decades based on modern numerical techniques for the field calculation and prototype testing (Jose F.d.O, 2000). This work is an attempt to compile much of the available information about the losses in the laminated cores and to elaborate the less loss but still in the practical tool for possible application in the transformer industry.

Mostly, the magnetic cores of the three phase transformers work under the alternating magnetisation but the different type of the magnetisation is produced in the T-joint of the three limb three phase transformers. It has been widely reported that in these regions, the magnetic material is subjected to the rotational magnetisation (Radley B., 1981, Kanada T., 1996). The magnetic excitation which produces the rotational and alternating magnetisation at arbitrary direction within the plane of the lamination is called as the two dimensional magnetisation. If the excitation causes the rotation of the flux density vector, then the magnetisation is also referred to as the rotational magnetisation. The core losses in the laminated cores are estimated to dissipate over 3% of all generated electricity (Moses A.J., 1992). The measurement of the power losses under the alternating magnetisation conditions are precisely defined by the international standards (IEC, 1996). It is attempted to measure the magnetic properties of the magnetic material under the circular flux density or magnetic field (Stanislaw Z., 2005). This study is focused on the stacked laminated cores and to suit an appropriate sample of tested units, restricted to the three phase three limb cores built from the grain oriented silicon of the high permeability steel at 50 Hz. The range of the flux densities chosen for the analysis is 1.0 T to 1.8 T. The intention of covering is not only the usual operating condition but also in the special cases where the low induction (1.0 T to 1.3 T) is required and also the temporary overfluxing with the transformer operating close to saturation levels (1.7 T to 1.8 T).

## 1.2. The Aim Of This Research

The aim of this research is to investigate the influence of the different cutting angle of T-joint on the power loss and flux distribution hence will found which type of the cutting angle of T-joint with the lowest power loss on the transformer core lamination.

In summary, the works have been done for this research are to design, develop and construct the 100kVA Distribution Transformer core model assembled with the Butt Lap joint, 60° T-joint, 45° T-joint and 23° T-joint. Method that use in the investigation is the No-Load Test by arrays of the search coil. The nominal power loss for the core material is measure using the Epstein Test Frame. From the result of the nominal power loss and the actual power loss measurement will be found the building factor for each transformer core model. The Single Sheet Tester was used to find the flux in the easy and hard direction. The localised power loss for each point in the lamination of each cores model has been measured by using the temperature rise technique with the thermistor. The path way of the flux travels in the core of each type of the T-joint was simulated by using the Finite Element Method of the QuickField software. The mesh and contour graph of the localised fundamental and harmonic flux density of T-joint core was drawn by using the Matlab software and also the mesh and contour graph of the localised power loss at each T-joint.

## Chapter Two

### Magnetic Properties, Flux Distributions And Losses

#### 2.1. Magnetic Properties Of Ferromagnetic Materials

The magnetic properties of a given material can be divided into two groups. The first group belongs to those properties such as the saturation magnetisation and the saturation magnetostriction. These properties are the fundamental constants with the ferromagnetic element or its alloy. The second groups are those properties which depend on the structure and previous history of a given material. The structure sensitive properties include the permeability, remanence, coercive force and magnetostriction.

The magnetic properties of the material can be described as the magnetisation and domain theory, magnetisation curve, demagnetising field, magnetocrystalline anisotropy, the magnetism and rotational magnetisation, the alternating magnetisation, the rotational magnetisation and the soft magnetic materials in the rotational magnetisation.

##### 2.1.1. The Magnetisation And Domain Theory

The magnetisation curve can be described in the terms of the domain theory. It is convenient to treat the curve in the three main parts and explain each part in terms of the domain theory (D. Jiles, 1996). Figure 2.1 shows the domain processes occurring as the material is magnetised to saturation. The first part called initial part which the domain process occurs which is a growth of domain which are align favourably with respect to the field and a consequent reduction in size of domains which are aligned in direction opposing the field. The second part called middle part which the mechanism becomes significant, this is domain rotation in which the atomic magnetic movements within an unfavourably aligned domain overcome the anisotropy energy and suddenly rotate from their original direction of magnetisation into one of the crystallographic easy axis which is nearest to the field direction. The third part called upper portion which the domain process coherent rotation takes

place. In this process the magnetic moments, which are aligned along the preferred easy axis lying close to the field direction are gradually rotated into the field direction as the magnitude of the field is increased. Figure 2.2 and 2.3 show the domain wall structure of the grain oriented silicon steel, M5 magnify by 500X and 300X.

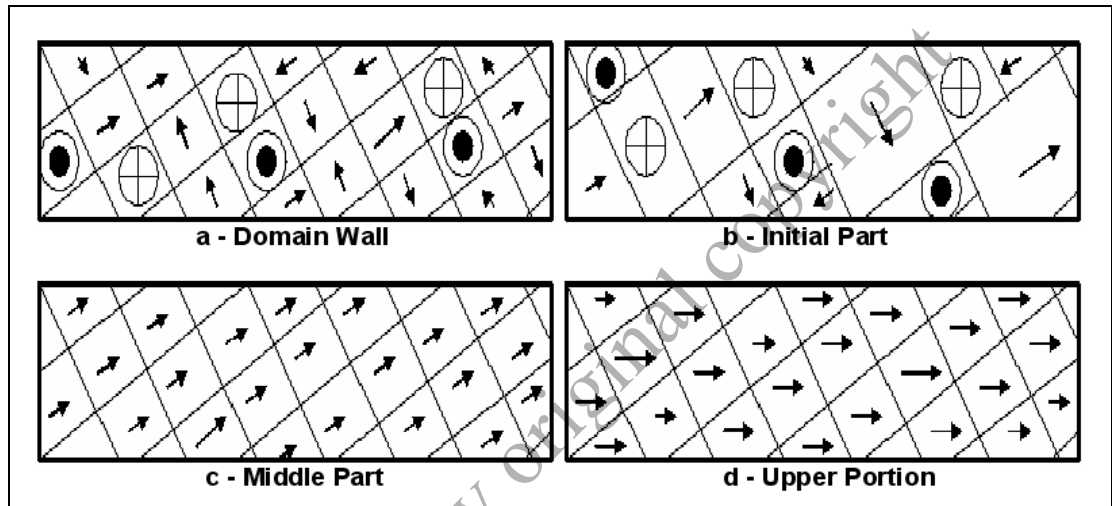


**Figure 2.1:** Domain processes occurring as the material is magnetised to saturation

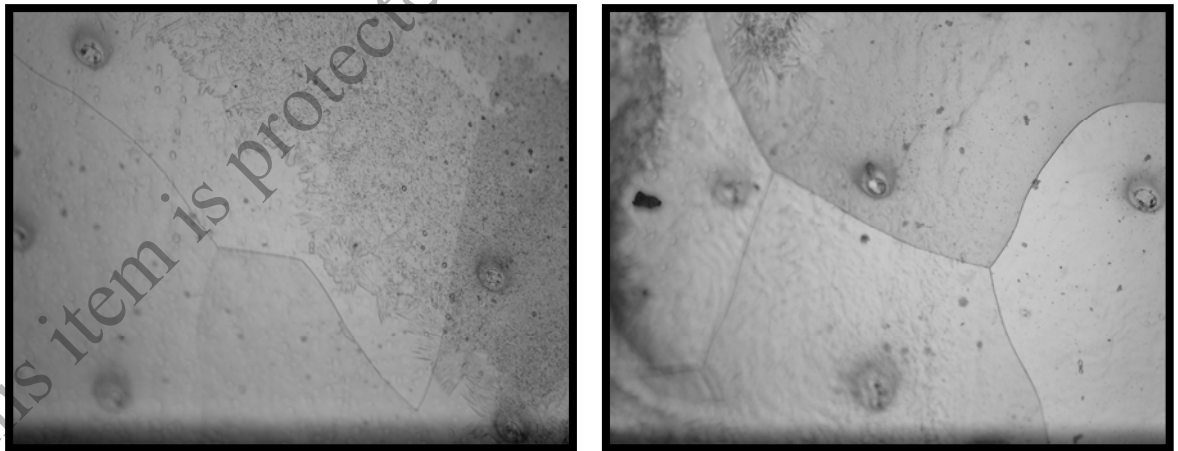


**Figure 2.2:** Domain wall structure of M5 magnify by 500X

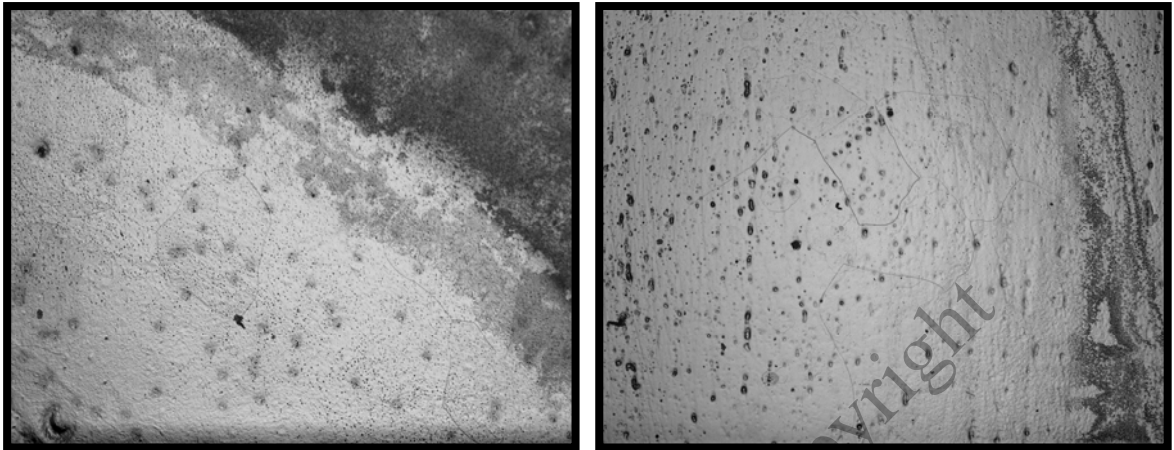


**Figure 2.3:** Domain wall structure of M5 magnify by 300X

### 2.1.2. Magnetisation Curve

The curve which relates the induction,  $B$  to the field strength,  $H$  is called the magnetisation curve. This curve is important because it can find the permeability,  $\mu$  at any values of the  $B$  or  $H$  as well as the initial and the maximum permeability which are often used for the comparative purposes. The permeability,  $\mu$  is the ratio of the  $B$  over  $H$ . The initial permeability ( $\mu_{in}$ ) is found from the slope of the B-H curve at the low fields. The maximum permeability ( $\mu_m$ ) is the maximum value found by dividing the  $B$  by  $H$ , graphically is the slope of the line from the origin to the point on the knee of the curve. At the large values of the  $H$ , the material becomes saturated and at the saturation limit the curve becomes the horizontal line (B.D. Cully, 1972). Figure 2.4 shows the  $B$  versus  $H$  curve of the ferromagnetic material.

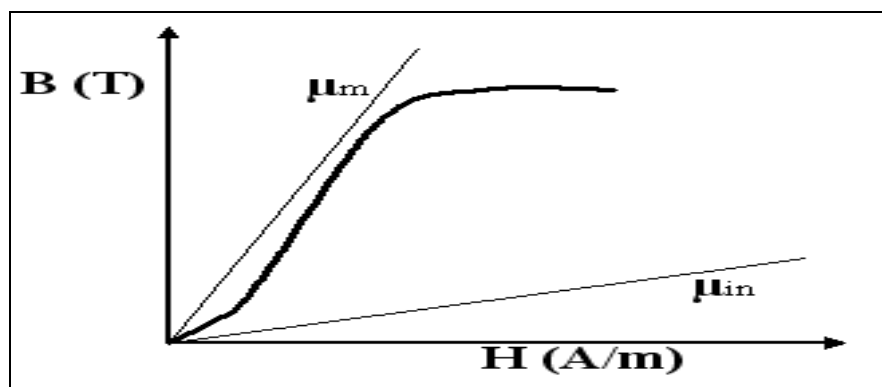


**Figure 2 4:** The B versus H curve of the ferromagnetic material

### 2.1.3. Demagnetising Field

It is necessary to consider the demagnetisation factor in the ferromagnetic materials. The exact internal field in the ferromagnetic material is made up of two parts,

$$H_{in} = H_{app} - H_d \quad (2.1)$$

Where  $H_{app}$  represents the applied magnetic field outside the specimen and  $H_d$  represents the demagnetising field and depend on the magnetisation in the material and the shape of the specimen [2.2]. It is expressed in

$$H_d = N_d M \quad (2.2)$$

$N_d$  is the demagnetising factor which is calculated from the sample geometry.

### 2.1.4. Magnetocrystalline Anisotropy

When the ferromagnetic material is subjected to an applied field, the observed magnetisation depends on the both magnitude of the field and the crystallographic direction along which it is applied. The large field of the magnetisation will reach the saturation value which is the same for all crystallographic directions. This shows that all magnetisation vectors have been rotated as to be parallel to the applied field. The crystallographic direction for which the magnetisation reaches saturation in the lowest applied field is known as the easy direction of magnetisation or the easy axis of magnetisation. This is the axis which the magnetisation vectors of the domains lay in the absence of an applied field (George L., 1998). Figure 2.5 shows the magnetisation curves in the various crystallographic directions to illustrate the magnetocrystalline anisotropy of the iron